

ARTICLE

High-Resolution Infrared-Vacuum Ultraviolet Photoion and Pulsed Field Ionization-Photoelectron Methods for Spectroscopic Studies of Neutrals and Cations

Xi Xing, Beth Reed, Mi Kyung Bahng, Peng Wang, Hin Koo Woo, Sun Jong Baek, Chee Shing Lam, Cheuk Yiu Ng*

Department of Chemistry, University of California, Davis, Davis, California 95616, USA

(Dated: Received on January 7, 2008; Accepted on January 25, 2008)

We show that by scanning the frequency of a single mode infrared (IR) optical parametric oscillator (IR-OPO) laser to excite the molecular species of interest and fixing the frequency of a vacuum ultraviolet (VUV) laser to photoionize the IR excited species, high-resolution IR spectra of polyatomic neutrals can be obtained with high sensitivity. The fact that this IR-VUV-photoion (IR-VUV-PI) method is based on VUV photoionization probe, and thus, allows the identification of the neutral IR absorber, makes it applicable for IR spectroscopy measurements of isotopomers, radicals, and clusters, which usually exist as impure samples. The highly resolved IR-VUV-PI measurements achieved using the single mode IR-OPO laser have made possible the selection of single rovibrational states of CH_3X ($\text{X}=\text{Br}$ and I), C_2H_4 , and C_3H_4 for VUV-pulsed field ionization-photoelectron (VUV-PFI-PE) measurements, resulting in rovibrationally resolved photoelectron spectra for these polyatomic molecules. These experiments show that the signal-to-noise ratios of the IR-VUV-PI and IR-VUV-PFI-PE spectra obtained by employing the high-resolution IR-OPO laser are significantly higher than those observed in previous IR-VUV-PI and IR-VUV-PFI-PE studies using a low-resolution IR-OPO laser. Further improvement in sensitivity of IR-VUV-PI and IR-VUV-PFI-PE measurements by using the collinear arrangement of IR-VUV lasers and molecular beam is discussed.

Key words: Vacuum ultraviolet, Infrared, Pulse-field photoelectron, High resolution

I. INTRODUCTION

The two-color infrared (IR)-vacuum ultraviolet (VUV) laser photoion (IR-VUV-PI) detection scheme has been demonstrated to be a sensitive technique for vibrational spectroscopy studies of molecular neutrals [1-11]. This method involves the setting of the VUV laser frequency below the ionization energy (IE) of the molecule of interest and scanning the IR laser to excite the vibrational bands of the molecule. Since the ion signal is observed only when the IR laser frequency matches an IR transition, the IR-VUV-PI spectrum thus recorded provides a good measure of the IR absorption spectrum for the neutral molecule. In IR-VUV-PI measurements of many small molecules, where the decay by intramolecular vibrational energy redistributions (IVRs) [12] is not important, the delay between the IR and VUV lasers can be set in the range from a few ns to a few μs . Excellent signal-to-noise ratios can be achieved in IR-VUV-PI measurements because of the high sensitivity of ion detection and the negligible ion background produced by the VUV laser [1-4,6-11]. The IR-VUV-PI method has the ability to identify the mass of the neutral IR absorber, and thus, is

suitable for IR spectroscopy measurements of reactive and cluster species, which usually coexist with other impure species. This represents a major advantage over the traditional Fourier transform IR method [13], which has no capability to identify the mass of the neutral IR absorber.

The supersonic molecular beam technique [14] has been widely used in photoelectron spectroscopy measurements to cool the neutral gaseous sample in order to reduce the thermal rotational and vibrational populations [1-11,15]. The cooling of a polyatomic molecular sample to a few degrees K by supersonic expansion has led to simplified pulsed field ionization-photoelectron (PFI-PE) spectra, allowing the observation of rotational structures for many polyatomic species. We have shown that by IR laser excitation, a single rovibrational state can be selected for photoionization efficiency (PIE) and PFI-PE studies [3,4,6-11]. From the point of view of a spectroscopic technique, the preparation of the molecule in a single rovibrational state by IR excitation is equivalent to cooling the molecule to 0 K such that only one (the lowest) rotational level is populated. Combining the structural and conformational selectivity of IR excitation and the detection sensitivity of VUV photoionization, the IR-VUV-PI and IR-VUV-PFI-PE methods are promising techniques for spectroscopic studies of neutrals and ions.

In our previous IR-VUV-PI and IR-VUV-PFI-PE studies of CH_3I and C_2H_4 [3,4,8], which used a low res-

* Author to whom correspondence should be addressed. E-mail: cyng@chem.ucdavis.edu

olution (optical bandwidth = 0.25 cm^{-1} (full-width at half-maximum, FWHM)) IR-optical parametric oscillator (IR-OPO) laser, the preparation of a single rotational level was not completely realized. In this work we report on the performance of IR-VUV-PI and IR-VUV-PFI-PE measurements using a single mode high-resolution IR-OPO laser with an optical bandwidth of 0.007 cm^{-1} (FWHM). With the improved resolution of the IR-OPO laser, it is possible to clearly resolve rotational transitions of selected vibration bands of CH_3Br , CH_3I , C_2H_4 , and C_3H_4 [9-11,16]. As a result, IR-VUV-PFI-PE measurements can be made on these polyatomic molecules prepared in single rovibrational states. These demonstration experiments show that the signal-to-noise ratios of the IR-VUV-PI and IR-VUV-PFI-PE spectra obtained by employing the high-resolution IR-OPO laser are significantly higher than those observed in previous studies using a low-resolution IR-OPO laser.

II. EXPERIMENTS

A. IR-VUV laser photoion-photoelectron apparatus

The IR-VUV-PI measurements for IR spectroscopy of neutral molecules and the IR-VUV-PFI-PE measurements for spectroscopy studies of their cations are made using the IR-VUV photoion-photoelectron apparatus [2-11]. Since the arrangement of this apparatus and procedures used for IR-VUV-PI and IR-VUV-PFI-PE measurements have been described in detail previously [5], they will be described only briefly below.

The IR-VUV photoion-photoelectron apparatus consists of a comprehensive tunable VUV laser (repetition rate of 30 Hz, tunable range of 7-19.5 eV, optical bandwidth of 0.12 cm^{-1}) based on nonlinear four-wave sum- and difference-frequency mixings in the rare gases (Ar, Kr, and Xe) and Hg vapor [3,4,17,18], a high-resolution, broadly tunable single mode IR-OPO laser, and a photoion-photoelectron apparatus [17,18], which is equipped with a molecular beam production system, an ion time-of-flight (TOF) mass spectrometer, and an electron TOF spectrometer. The output of the VUV and IR lasers are continuously monitored by wavemeters during the experiment for the purpose of frequency calibration. The VUV laser system is equipped with a Raman shifter in H_2 (D_2 , or CH_4) to extend the tunable range of ω_2 , such that the full VUV range of 7-19.5 eV can be generated without energy gaps. The optical bandwidth of the VUV radiation thus generated has been measured to be 0.12 cm^{-1} (FWHM) [17,18]. The VUV sum-frequencies or difference-frequencies of interest are selected by a windowless VUV monochromator before intersecting the gas sample beam at 90° in the photoionization region of the photoionization chamber. The electrons and ions thus formed are detected by microchannel plate (MCP) detectors of the electron and

ion TOF spectrometers. After passing through the photoionization region, the intensity of the VUV beam is measured by a copper photoelectric detector, such that the measured photoion and PFI-PE intensities can be normalized by the corresponding VUV intensities.

The IR laser system used is a single mode IR-optical parametric oscillator (IR-OPO) (Laser Vision) pumped by the 1064 nm output of an injection seeded Nd:YAG laser (pulsed energy = 550 mJ) operated at 15 Hz. The stabilization of the single mode operation is maintained by a piezo located on the rear mirror of the oscillator. The voltage on the piezo can be adjusted either manually or automatically according to the feedback from the etalon rings displayed on a monitor. The IR-OPO laser system is tunable in the range of 1.35-5.0 μm ($7407\text{--}2000\text{ cm}^{-1}$) with typical pulse energies in the range of 5-12 mJ at full power and a specified optical bandwidth of 0.007 cm^{-1} (FWHM). For most experiments presented here, the IR pulse energies used were in the range of 1-4 mJ at $\approx 3\text{ }\mu\text{m}$. A spherical lens of 1-m focal length is used to slightly focus the IR laser beam, resulting in a spot size of $\approx 2\text{ mm}\times 4\text{ mm}$ at the photoionization region.

The gaseous sample is generally premixed with a rare gas (He or Ar) before introducing into the photoionization region as a pulsed supersonic molecular beam. The pulsed beam is formed through a pulsed valve (General valve, nozzle diameter of 0.5 mm, repetition rate of 30 Hz) and is skimmed by a conical skimmer prior to intersecting the VUV laser beam perpendicularly at the photoionization region. During the experiment, the photoionization chamber and the ion TOF mass spectrometer are maintained at pressures of $\approx 10^{-5}\text{ Pa}$.

The timing sequence for opening of the pulsed valve, firing of the IR and VUV lasers, and applying the PFI field is controlled by two digital delay units (Stanford Research DG535). The photoion and photoelectron signals from the MCP detectors are pre-amplified and integrated by independent boxcar integrators before processing by a personal computer.

B. VUV-PIE and VUV-PFI-PE measurements

The procedures for VUV-PIE and VUV-PFI-PE measurements have been described in detail previously, and thus, will not be reiterated here [17,18]. Briefly, for VUV-PIE measurements, a DC field $\approx 40\text{ V/cm}$ is maintained at the repeller region to extract the photoions into the TOF mass spectrometer for detection by the ion MCP detector. For VUV-PFI-PE measurements, a DC field of 0.1 V/cm is applied to disperse the prompt background photoelectrons. After a delay of 1 μs with respect to the VUV laser pulse, a pulsed field of 0.3 V/cm is applied to ionize the high- n Rydberg molecules and to extract the PFI-PEs toward the electron MCP detector. The PFI-PE resolutions achieved

in the present study are 1.2-1.5 cm^{-1} (FWHM). These achievable resolutions are only sufficient for resolving vibrational transitions in VUV-PFI-PE measurements of polyatomic molecules such as CH_3X ($\text{X}=\text{Br}$ and I), C_2H_4 , and C_3H_4 . To determine rovibrationally resolved VUV-PFI-PE spectra for these molecules is the main theme of this article.

C. IR-VUV-PI measurements

As described above, the VUV laser radiation selected by the windowless VUV monochromator intersects with the sample molecular beam at 90° in the photoionization region. The molecular beam axis lies in the plane defined by the axes of the monochromator entrance and exit arms (or the Roland circle) and is perpendicular to the exit arm of the VUV monochromator. Two configurations have been used for the IR-VUV-PI measurements. The first configuration involves the introduction of the IR laser beam into the photoionization region counter propagating with the VUV laser beam. When the optimal spatial overlap of the IR and VUV laser beams is achieved at the photoionization region, the IR laser beam can pass through the monochromator and exit its entrance arm. In the second configuration, the IR laser beam enters the photoionization region along the molecular beam axis. In both configurations, the optimal overlap of the IR, VUV, and molecular beams can be monitored by the photoion signal. All IR-VUV-PI data presented here have been obtained using the first experimental configuration.

In IR-VUV-PI measurements, the VUV laser frequency is usually set at $\approx 100 \text{ cm}^{-1}$ below the IE of the molecule such that the VUV alone is insufficient to ionize the molecule. However, a small background signal of the molecular ions can be produced due to thermal populations of the molecules in excited rovibrational states. The fact that the repetition rate (30 Hz) for the VUV laser is by design twice that (15 Hz) of the IR-OPO laser allows the shot-to-shot subtraction of this ion background. The application of the VUV laser pulse is delayed by 50-100 ns with respect to the IR laser pulse. The IR-VUV-PI spectra are obtained by scanning the IR laser to cover the frequency range of the vibrational band of interest. Although the single mode IR-OPO laser is specified to have an optical bandwidth of 0.007 cm^{-1} (FWHM), the best measured spectral resolution is $\approx 0.012 \text{ cm}^{-1}$ (FWHM), which is observed in a photoacoustic measurement of CH_4 in the mid-IR using a room temperature CH_4 gas cell (260-650 Pa). A small contribution to the IR absorption linewidth observed in the latter experiment due to the Doppler broadening effect is to be expected. As shown below, the achieved resolution for IR-VUV-PI measurements presented in this study using the single mode IR-OPO laser is $\approx 0.02 \text{ cm}^{-1}$ (FWHM), suggesting that some broadening may have been arisen from VUV photoionization processes [9].

toionization processes [9].

1. CH_3X ($\text{X}=\text{Br}$ and I)

Figure 1 (a) and (b) compare the IR-VUV-PI spectra for the $\nu_1=1$ (C-H stretching) vibrational band of CH_3Br using the high and low resolution IR-OPO laser, respectively. This is a parallel band with the $\Delta J=0, \pm 1$ and $\Delta K=0$ selection rules, resulting in the normal rotational structure of the P-, Q-, R-branches. The assignments of rotational transitions are marked on top of the spectra. The different K' -transitions are well resolved in the high resolution scan, while only individual J' -transitions are resolved in the low resolution spectrum. The two spectra shown in Fig.1(a) are the high resolution (J', K') resolved IR spectra of the ν_1 bands of $\text{CH}_3\text{Br}^{79}$ and $\text{CH}_3\text{Br}^{81}$. A slight shift in frequency for the IR-VUV-PI spectra of $\text{CH}_3\text{Br}^{79}$ and $\text{CH}_3\text{Br}^{81}$ is observed. Since the low resolution scan is unable to differentiate rotational transitions originating from $\text{CH}_3\text{Br}^{79}$ and $\text{CH}_3\text{Br}^{81}$, only the IR-VUV-PI spectrum for $\text{CH}_3\text{Br}^{79}$ is plotted in Fig.1(b). The spectral simulation of these spectra shows a rotational temperature of 8 K for the CH_3Br beam. At this temperature, the CH_3Br molecules are predominantly in the $K''=0$ or 1 rotational states with a very small portion at $K''=2$ or higher levels. The spectra for $\text{CH}_3\text{Br}^{79}$ and $\text{CH}_3\text{Br}^{81}$ illustrate an important merit of the IR-VUV-PI technique for IR spectroscopic measurements. The fact that the IR absorber is detected by photoionization mass spectrometry makes it applicable for IR spectroscopic measurements of isotopomers, reactive radicals, and clusters, which usually exist as impure samples.

The high-resolution, (J', K')-resolved IR-VUV-PI spectrum for the CH_3I ($\nu_1=1$) vibrational band has also been obtained using the single mode IR-OPO laser (not shown here) for comparison with that reported previously [3] using the low resolution IR-OPO laser.

2. C_2H_4

We have measured the IR-VUV-PI spectra for the $\nu_{11}(\text{b}_{1\text{u}})$, $\nu_2+\nu_{12}(\text{b}_{1\text{u}})$, and $\nu_9(\text{b}_{2\text{u}})$ vibrational bands of ethylene, where $\nu_2(\text{a}_g)$, $\nu_9(\text{b}_{2\text{u}})$, $\nu_{11}(\text{b}_{1\text{u}})$, and $\nu_{12}(\text{b}_{1\text{u}})$ represent the respective C-C stretching, CH_2 stretching, CH_2 stretching, and CH_2 bending modes of $\text{C}_2\text{H}_4(\tilde{X}^1\text{A}_g)$. As an example, we show in Fig.2 and Fig.3 the IR-VUV-PI spectra of the $\nu_2+\nu_{12}$, and ν_9 bands, respectively. The vibrational bands shown in Fig.2(a) and Fig.3(a) are high-resolution spectra recorded using the single mode IR-OPO laser, whereas those of Fig.2(b) and Fig.3(b) were recorded previously [8] by using the low resolution IR-OPO laser. Comparing the observed rotational linewidths in the present and previous IR-VUV-PI measurement, we conclude that the resolution achieved in the single mode

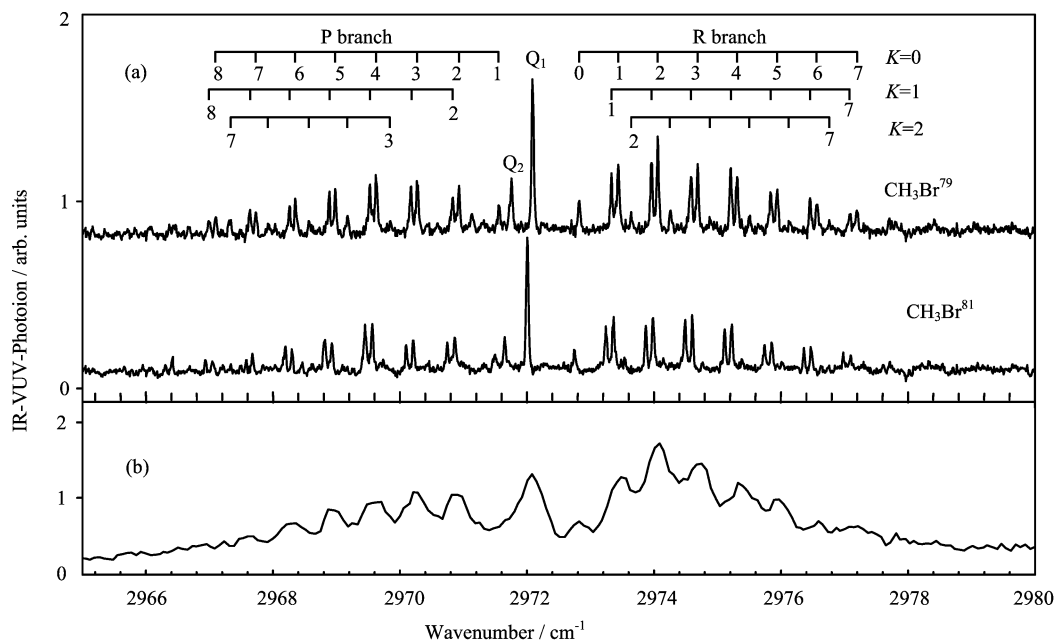


FIG. 1 IR-VUV-PI spectra for the $\nu_1=1$ (C-H stretching) vibrational band of (a) $\text{CH}_3\text{Br}^{79}$ (upper spectrum) and $\text{CH}_3\text{Br}^{81}$ (lower spectrum) obtained using the high resolution single mode IR-OPO laser and (b) $\text{CH}_3\text{Br}^{79}$ obtained using the lower resolution IR-OPO laser. Rotational assignments are marked on top of the spectra in (a). The resolutions achieved in the high and low resolution measurements are 0.02 and 0.25 cm^{-1} (FWHM), respectively.

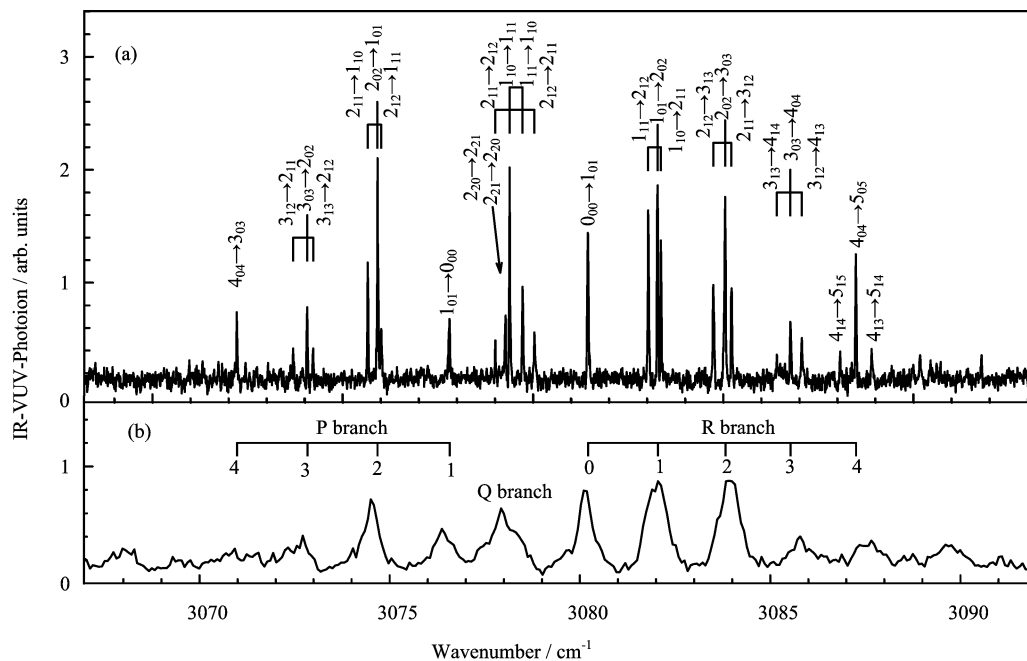


FIG. 2 (a) IR-VUV-PI spectrum of C_2H_4 (\tilde{X}^1A , $\nu_2+\nu_{12}$) in the IR frequency range of $3067\text{-}3092 \text{ cm}^{-1}$ recorded by using (a) the single mode IR-OPO laser and (b) the low resolution IR-OPO laser. The assignment of the rotational transitions $N''K_a''K_c'' \rightarrow N'K_a'K_c'$ are marked on top of the spectrum plotted in (a), where (N'', K_a'', K_c'') and (N', K_a', K_c') are the respective rotational quantum numbers for the ground vibrational state and the $\nu_2+\nu_{12}$ excited state of C_2H_4 . The spectrum of (b) exhibits the P-, Q-, and R-branches. The assignment of the $P(N'')$, $Q(N'')$, and $R(N'')$ rotational lines are marked on top of (b). The resolutions achieved in the high and low resolution measurements are 0.02 and 0.25 cm^{-1} (FWHM), respectively.

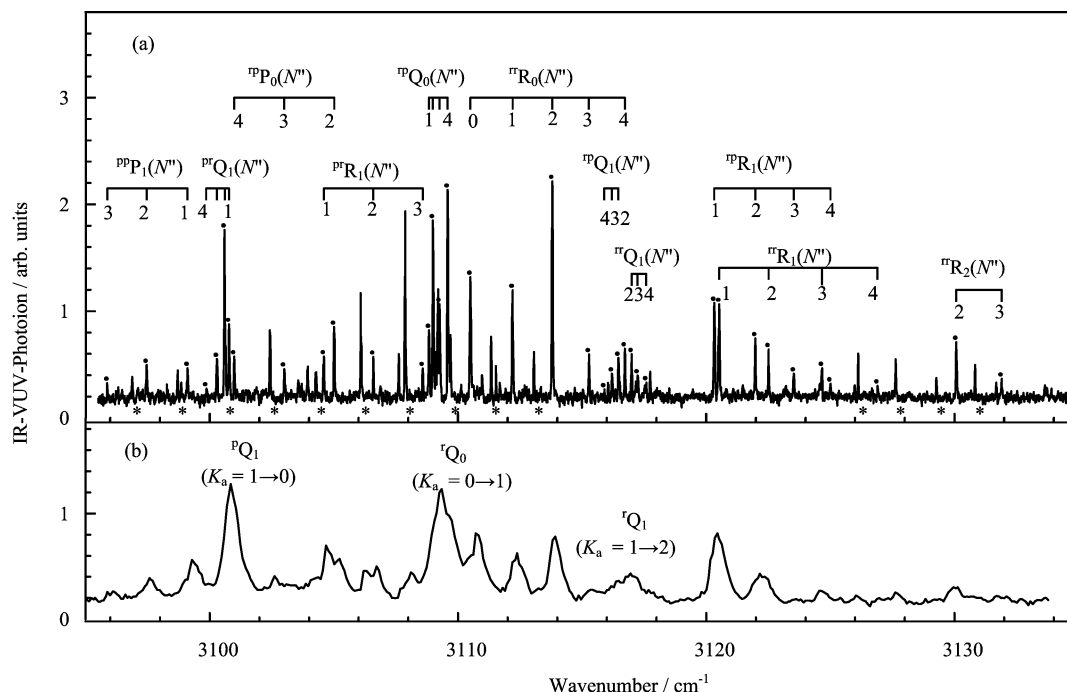


FIG. 3 IR-VUV-PI spectrum of C₂H₄ (\tilde{X}^1A, ν_9) in the IR frequency range of 3095-3135 cm⁻¹ recorded by using (a) the single mode IR-OPO laser and (b) the low resolution IR-OPO laser. The rotational transitions are marked as $\Delta K'_a \Delta K'_c \Delta N'_{K''} (N'')$ on top of the spectrum, where $\Delta K'_a = K'_a - K''_a$ and $\Delta K'_c = K'_c - K''_c$ with values of -1 and 1 are denoted as p and r, respectively. The assigned peaks are marked by solid dots on top of the peaks, while the extra peaks originated from other vibrational bands are marked by asterisks below the peaks. The resolutions achieved in the high and low resolution measurements are 0.02 and 0.25 cm⁻¹ (FWHM), respectively.

IR-VUV-PI measurements of Fig.2(a) and Fig.3(a) is more than 12-fold higher than that observed in the low-resolution spectra of Fig.2(b) and Fig.3(b).

The IR-VUV-PI vibrational band for the $\nu_2 + \nu_{12}$ measured in range of 3067-3092 cm⁻¹ (Fig.2) is an A-type transition band, where the selection rules: $\Delta N' = N' - N'' = 0, \pm 1$, $\Delta K'_a = K'_a - K''_a = 0$ and $\Delta K'_c = K'_c - K''_c = 1$ are valid [8]. As marked on top of Fig.2(b), the low resolution spectrum exhibits the typical P-, Q-, and R-branches. The comparison of Fig.2(a) and Fig.2(b) shows that the Q-branch and many of the P(N'') and R(N'') lines observed in Fig.2(b) consist of multiple unresolved transition lines. The assignments of the allowed $N''_{K''_a K''_c} \rightarrow N'_{K'_a K'_c}$ rotational transitions are marked on top of Fig.2(a), where (N'', K''_a, K''_c) and (N', K'_a, K'_c) are rotational quantum numbers for the respective ground and excited vibrational states of C₂H₄.

After taking into account the nuclear spin statistical weights of the rotational levels, the simulation of the spectrum of Fig.2(a) indicates that the rotational temperature of the C₂H₄ sample achieved in the supersonic expansion is 8-10 K [8]. As a result, more than 95% of the molecules are expected to populate the rotational levels $N'' < 5$ of the ground state. For ethylene in its vibronic ground state, the nuclear spin statisti-

cal weights are 7, 3, 3, and 3 for $K_a K_c = ee, eo, oe,$ and oo , respectively, where e and o stand for even and odd. The largest nuclear spin statistic weight for the $K_a K_c = ee$ levels contributes to the outstanding intensities for the transitions of $2_{02} \rightarrow 1_{01}$ in P(2), $0_{00} \rightarrow 1_{01}$ in R(0), and $2_{02} \rightarrow 3_{03}$ in R(2) transitions of the $\nu_2 + \nu_{12}$ and ν_{11} bands.

The IR-VUV-PI spectra of the C₂H₄ (\tilde{X}^1A_g, ν_9) band (Fig.3) are governed by the selection rules of the B-type IR transitions: $\Delta N' = 0, \pm 1$, $\Delta K'_a = \pm 1$, and $\Delta K'_c = \pm 1$ [8]. Thus, the rotational structures are quite different from those of the ν_{11} and $\nu_2 + \nu_{12}$ bands, which have nearly identical rotational structures because they are governed by the same rotational selection rules. The IR-VUV-PI band of ν_9 consists of three overlapping sub-bands, which are classified by $\Delta K'_a = 0 \leftarrow -1$, $\Delta K'_a = 1 \leftarrow 0$, and $\Delta K'_a = 2 \leftarrow -1$ transitions. Each of these sub-bands comprises of the P-, Q-, and R-branches. The comparison of Fig.3(a) and Fig.3(b) reveals that many of the rotational peaks resolved in the Fig.3(b) correspond to single rotational transitions. This observation can be ascribed to the relatively large separations of the K'_a levels. The rotational assignments marked on top of Fig.3(a) are designated as $\Delta K'_a \Delta K'_c \Delta N'_{K''} (N'')$, where $\Delta K'_a$ and $\Delta K'_c$ with values of -1 and 1 are denoted as p and r, respectively. All rotational lines that are assigned are marked by a black dot on top of the peaks. Some

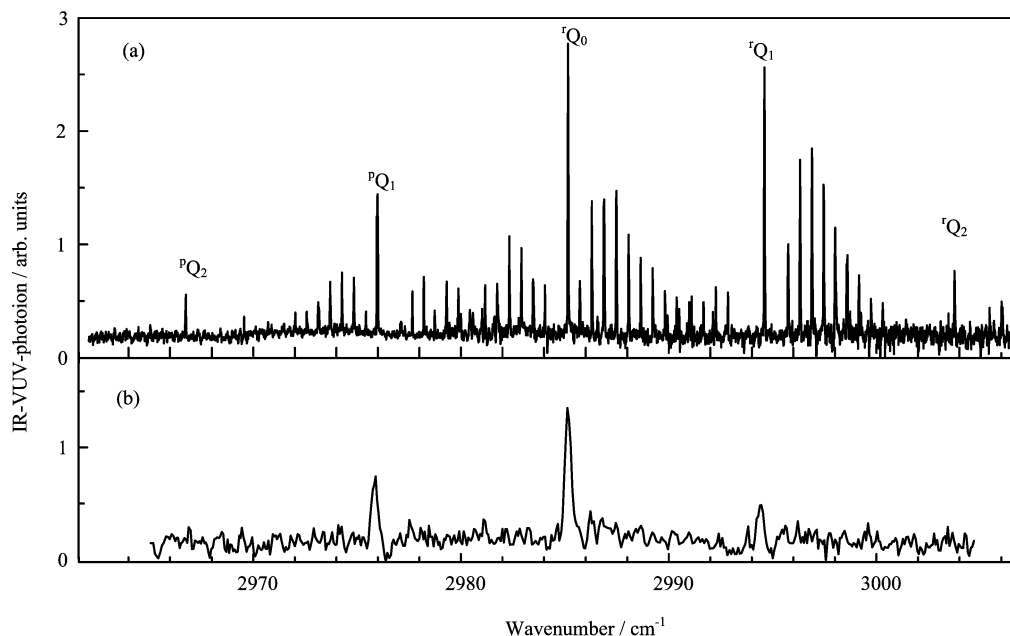


FIG. 4 IR-VUV-PI spectra of $C_3H_4(\nu_6=1)$ band in the IR range of $2965\text{--}3005\text{ cm}^{-1}$ recorded by using (a) the single mode IR-OPO laser and (b) the low resolution IR-OPO laser. The rotational transitions in the Q-branches ($\Delta N'=N'-N''=0$) are marked as $^{\Delta K'}Q_{K''}$ on top of the spectrum, where, $\Delta K'=K''-K'$ with values of -1 and 1 are denoted as p and r, respectively. The resolutions achieved in the high and low resolution measurements are 0.02 and 0.25 cm^{-1} (FWHM), respectively.

extra lines observed in Fig.3(a) that are not predicted by the spectral simulation of the band are marked by asterisks under the peaks. These peaks are found to be equally spaced by $\approx 1.7\text{ cm}^{-1}$, indicating the existence of other A-type vibrational bands in this energy region.

3. C_3H_4

We have also measured the IR-VUV-PI spectra for the C–H stretching vibration bands of C_3H_4 , including ν_1 (acetylenic C–H stretch) [8], ν_2 (symmetric CH_3 stretch) [9], and ν_6 (anti-symmetric CH_3 stretch). The ν_1 band (not shown here) is a parallel transition band, exhibiting the usual P-, Q-, and R-branches. Since the rotational constant for the ground state is very close to that for the $\nu_1=1$ excited state, the $K' \leftarrow K''=0 \leftarrow 0$ and $1 \leftarrow 1$ transitions cannot be resolved in these spectra. The simulation of the IR-VUV-PI spectrum of the ν_1 band indicates a rotational temperature of $\approx 8\text{ K}$ for the supersonically cooled C_3H_4 sample. At such a rotational temperature, C_3H_4 molecules mostly populate in the lowest $K''=0$ and 1 states with nearly equal intensities.

Figure 4 (a) and (b) depict the ν_6 band obtained using the single mode IR-OPO and the low resolution IR-OPO laser system, respectively. The ν_6 band is a perpendicular band governed by the $\Delta J=0, \pm 1$ and $\Delta K=\pm 1$ selection rules, and is shown in the high resolution spectrum of Fig.4(a) to consist of five sub-bands.

Each sub-band consists of a prominent Q($\Delta J=0$) and the P($\Delta J=-1$) and R($\Delta J=1$) branches. In comparison, only three Q bands are discernible in the low resolution spectrum of Fig.4(b). Furthermore, the P($\Delta J=-1$) and R($\Delta J=1$) branches for the sub-bands resolved in Fig.4(a) are indiscernible in Fig.4(b). This observation indicates that the increase in IR resolution by using the high-resolution IR-OPO laser actually enhances the sensitivity of IR-VUV-PI measurements.

D. IR-VUV-PFI-PE measurements

The IR-VUV-PI measurements presented above are required for IR-VUV-PFI-PE measurements to be presented below. The higher sensitivity in IR-VUV-PI measurements is shown to translate directly into improved sensitivity for IR-VUV-PFI-PE measurements.

1. CH_3X ($X=Br$ and I)

Using the low resolution IR-OPO laser, we have previously recorded the IR-VUV-PFI-PE spectra for the CH_3I ($\nu_1=1$) band with selected rotational levels, $J'=1, 2, 5, 7,$ and 10 [3]. In the latter experiment, since $K'=0$ and 1 are not resolved in the low resolution IR-VUV-PI spectrum, individual J' transitions consist of at least two transitions from the $K'=0$ and 1 states. By fixing the high-resolution IR-OPO laser at individual ro-

tational transitions in the K-stack of the R-branch of the ν_1 band, we have obtained the IR-VUV-PFI-PE spectra for the $\text{CH}_3\text{I}^+(\tilde{X}^2\text{E}_{3/2}; \nu_1^+=1) \leftarrow \text{CH}_3\text{I}(\tilde{X}^1\text{A}_1, \nu_1=1)$ band with (J', K') prepared at (3,0), (4,0), (4,1), (5,0), (5,1), (6,0), (6,1), (7,0), and (8,0) [16]. As an example to illustrate that the PFI-PE spectra for $\text{CH}_3\text{I}(\tilde{X}^1\text{A}_1, \nu_1=1)$ prepared in single (J', K') states can be measured with good signal-to-noise ratios, we show the IR-VUV-PFI-PE spectra for (3,0) and (7,0) in Fig. 5(a) and 5(b), respectively. For a given J' value, almost identical rotational structures are observed in the IR-VUV-PFI-PE spectra for $K'=0$ and 1, except for a minor difference in their intensities [16]. The observation of identical rotational structures for $K'=0$ and 1 is consistent with the fact that the photoionization transitions, $P^+=1/2 \leftarrow K'=0$ and $P^+ = -1/2, 3/2 \leftarrow K'=1$, overlap with each other in the spectra, where $P^+ = K^+ + 1/2$. The similar intensities observed for the $K'=0$ and 1 transitions indicate that the photoionization cross sections are only weakly dependent on K' [16].

The rotationally selected and resolved IR-VUV-PFI-PE spectra for $\text{CH}_3\text{Br}(\nu_1)$ have also been obtained. These spectra, together with the analysis of state-to-state photoionization cross sections determined for CH_3X ($\text{X}=\text{Br}$ and I) will be published in a separate article [16].

2. C_2H_4

In the previous IR-VUV-PFI-PE study, we have obtained the IR-VUV-PFI-PE spectra [shown as curves (v) in Fig.6 for the $\nu_{11} \rightarrow \nu_2^+ + \nu_{12}^+$ photoionization band by exciting the P(2), R(1), and R(2) lines of the ν_{11}^+ band using the low resolution IR-OPO laser [4,8]. The P(2), R(1), and R(2) lines thus observed consist of unresolved transitions from three rotational levels, i.e., the 1_{01} level via $2_{02} \rightarrow 1_{01}$, the 1_{10} level via $2_{12} \rightarrow 1_{10}$, and the 1_{11} level via $2_{12} \rightarrow 1_{11}$, for P(2); the 2_{02} level via $1_{01} \rightarrow 2_{02}$, the 2_{11} level via $1_{10} \rightarrow 2_{11}$, and the 2_{12} level via $1_{11} \rightarrow 2_{12}$, for R(1); and the 3_{03} level via $2_{02} \rightarrow 3_{03}$, the 3_{12} level via $2_{11} \rightarrow 3_{12}$, and the 3_{13} level via $2_{12} \rightarrow 3_{13}$, for R(2). Using the high resolution single mode IR-OPO laser, each of these rotational levels can be distinctly selected for VUV-PFI-PE measurements [11]. The IR-VUV-PFI-PE spectra obtained using the single mode IR-OPO laser with C_2H_4 (ν_{11}) prepared in individual $N'_{K'_a K'_c} = 1_{01}, 1_{10}, 1_{11}, 2_{02}, 2_{11}, 2_{12}, 3_{03}, 3_{12}$, and 3_{13} rotational levels are plotted as curves (i), (ii), and (iii) in Fig.6. In order to show the relative intensities for the rotational transitions, the vertical scales of these spectra have the same $I_{(\text{PFI-PE})}/I_{(h\nu)}$ units, where $I_{(\text{PFI-PE})}$ and $I_{(h\nu)}$ represent the PFI-PE and VUV intensities, respectively. As expected, the structures of the lower resolution IR-VUV-PFI-PE spectra (curves (v) of Fig.6)] are different from their respective individual, high-resolution spectra (curves (i), (ii), and

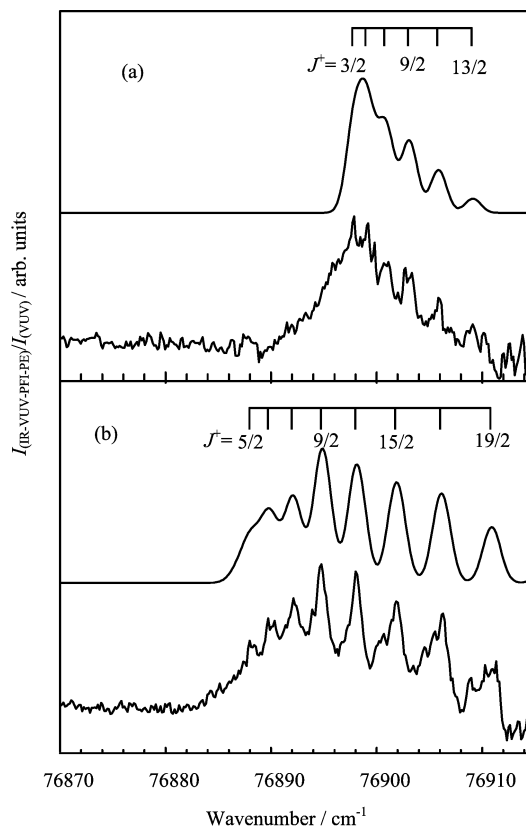


FIG. 5 (J', K') selected IR-VUV-PFI-PE spectra (lower curves) for $\text{CH}_3\text{I}^+(\tilde{X}^2\text{E}_{3/2}, \nu_1^+) \leftarrow \text{CH}_3\text{I}(\tilde{X}^1\text{A}_1, \nu_1)$ obtained by using the single mode IR-OPO laser to select the rotational levels: (a) $J'=3, K'=0$, and (b) $J'=7, K'=0$. The upper curves represent the simulated spectra. The rotational assignments ($J', K'=0 \rightarrow J^+, P^+=1/2$) are marked on top of the spectra.

(iii)), but have contributions from the corresponding high-resolution spectra. Curves (iv) of Fig. 6(a), 6(b), and 6(c) are the sum spectra obtained by adding the $1_{01}, 1_{10}$, and 1_{11} spectra of Fig.6(a), the $2_{02}, 2_{11}$, and 2_{12} spectra of Fig.6(b), and the $3_{03}, 3_{12}$, and 3_{13} spectra of Fig.6(c), respectively. As shown in these figures, the sum spectra are in excellent agreement with the corresponding low resolution [4,8] IR-VUV-PFI-PE spectra, i.e., curves (v). Furthermore, the sum spectra are shown to have significantly higher signal-to-noise ratios than the low resolution [4,8] IR-VUV-PFI-PE spectra.

In addition, we have measured the IR-VUV-PFI-PE spectra for the ionization transitions, $\text{C}_2\text{H}_4^+(\tilde{X}^2\text{B}_{3u}, \nu_i^+, N'_{K'_a K'_c}) \leftarrow \text{C}_2\text{H}_4(\tilde{X}^1\text{A}_g, \nu_{11}=1, N'_{K'_a K'_c}=3_{03})$ in a broad VUV frequency range using the single mode IR-OPO laser [8,11]. A total of 24 vibrational bands are identified in this measurement [11], whereas only the 7 strongest bands have been observed in the previous IR-VUV-PFI-PE study using the lower resolution IR-OPO laser [8], illustrating that the sensitivity of IR-VUV-PFI-PE measurements using the high-resolution

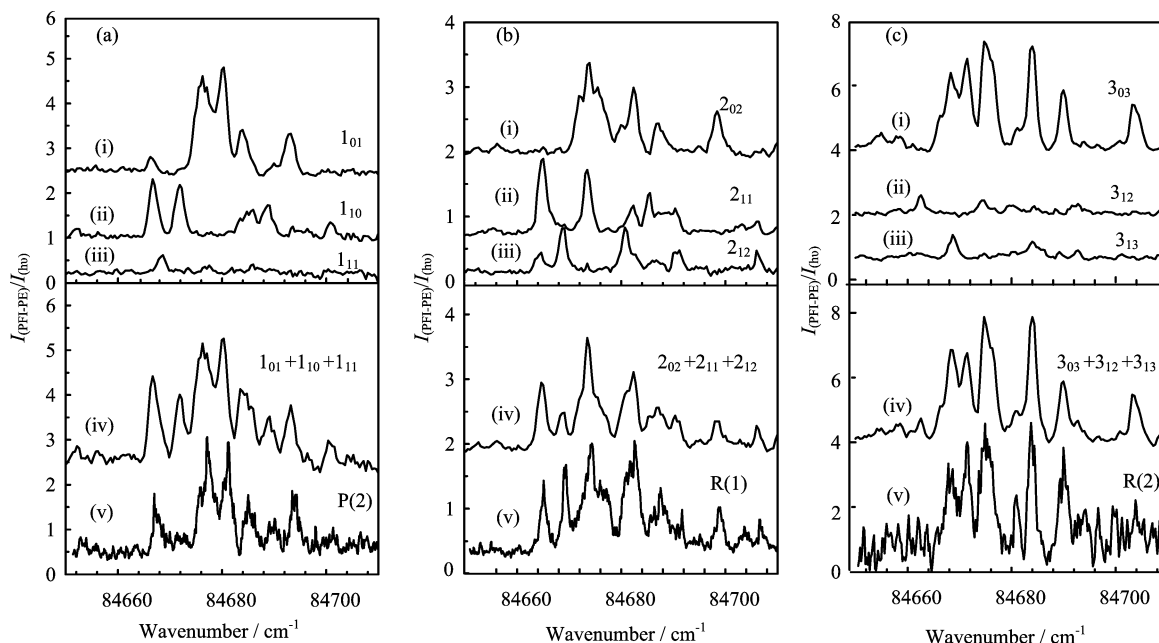


FIG. 6 IR-VUV-PFI-PE spectra of the $C_2H_4^+(\tilde{X}^2B_{3u}, \nu_2^+ + \nu_{12}^+, N_{K_a^+ K_c^+}^+ \leftarrow C_2H_4(\tilde{X}^1A_g, \nu_{11}, N_{K_a^+ K_c^+}')$ transitions in the VUV frequency range of 84650-84730 cm^{-1} obtained using the single mode IR-OPO laser. Here, the rotational levels, $N_{K_a^+ K_c^+}' = 1_{01}, 1_{10}, 1_{11}, 2_{02}, 2_{11}, 2_{12}, 3_{03}, 3_{12}, 3_{13}$ of ν_{11} are selected by fixing the IR-OPO laser at the corresponding transitions, $2_{02} \rightarrow 1_{01}, 2_{12} \rightarrow 1_{10}, 2_{12} \rightarrow 1_{11}, 1_{01} \rightarrow 2_{02}, 1_{10} \rightarrow 2_{11}, 1_{11} \rightarrow 2_{12}, 2_{02} \rightarrow 3_{03}, 2_{11} \rightarrow 3_{12}, 2_{12} \rightarrow 3_{13}$, which are resolved in the high-resolution IR-VUV-PI spectrum of ν_{11} (see the text). The IR-VUV-PFI-PE spectra thus observed are shown as curves (i), (ii), (iii) in (a), (b), and (c). The PFI-PE intensities ($I_{(PFI-PE)}$) have been normalized by the VUV intensity ($I_{(hv)}$) and have the same units for all figures. Curves (iv) of (a), (b), and (c) are the synthesized spectra obtained by adding the $1_{01}, 1_{10},$ and 1_{11} spectra of (a); the $2_{02}, 2_{11},$ and 2_{12} spectra of (b); and the $3_{03}, 3_{12},$ and 3_{13} spectra of (c), respectively. Curves (v) of (a), (b), and (c) are the IR-VUV-PFI-PE spectra obtained previously [8] by using the low resolution IR-OPO laser to selected the P(2), R(1) and (R2) rotational lines of the ν_{11} band.

single mode IR-OPO laser is enhanced compared to that using the low resolution IR-OPO laser. We have also performed IR-VUV-PFI-PE measurements of $C_2H_4(\nu_9)$ prepared in selected rovibrational levels by using the single mode IR-OPO laser (not shown here).

3. C_3H_4

The IR-VUV-PFI-PE spectra for the $C_3H_4^+(\nu_1^+, J_{K^+}^+) \leftarrow C_3H_4(\nu_1, J_{K'}')$ photoionization band (not shown here) have been measured by setting the single mode IR-OPO laser at individual rotational transitions, P(1), P(2), R(1), R(2), R(3), and R(4) resolved in the IR-VUV-PI spectrum of the $C_3H_4(\nu_1)$ band, which correspond to the preparation of respective rotational levels $J'=0, 1, 2, 3, 4,$ and 5 [10]. The simulation of the rovibrationally selected and resolved IR-VUV-PFI-PE spectra thus obtained has yielded highly precise values for the IE of the photoionization transition $C_3H_4^+(\tilde{X}^2E_{1/2}, \nu_+ = 1) \leftarrow C_3H_4(\tilde{X}^1A_1, \nu_1 = 1)$, the spin-orbit constant for $C_3H_4^+(\tilde{X}^2E, \nu_1^+ = 1)$, and the vibrational frequency for $C_3H_4(\nu_1^+)$. Furthermore, state-to-state cross sections for photoionization transitions originating from

$J'=0-5$ with $K'=0$ and 1 have been determined from the rotational analysis of IR-VUV-PFI-PE spectra for the $\nu_1^+ = 1 \leftarrow \nu_1 = 1$ band [10]. The IR-VUV-PFI-PE measurements of $C_3H_4(\nu_2$ and $\nu_6)$ prepared in selected rovibrational levels by using the single mode IR-OPO laser have also been made [16].

III. DISCUSSION

In the demonstration experiments presented here, we have focused on the IR measurements of the C-H stretching vibrational bands of several simple polyatomic molecules at around 3 μm . However, this method should not be limited to the study of the C-H vibrational modes. The current tunable range of the single mode IR-OPO laser is 1.35-5.0 μm . The wavelength extension down to 16 μm ($625 cm^{-1}$) based on the silver-gallium-selenide crystal ($AgGaSe_2$) can be obtained. Although the IR pulse energies in this long wavelength range are low ($\approx 0.1 mJ/pulse$ at $900 cm^{-1}$), the high-resolution output of the IR-OPO may still be able to saturate the IR transitions of some vibrational modes. The use of this extension unit would allow spectroscopy studies of chemically interesting vibrational

modes such as C–C stretching modes, which are in the range of $\approx 900\text{ cm}^{-1}$. The IR-VUV-PI experiments of this study indicate that the IR-VUV-PI method has the sensitivity for IR spectroscopy studies of radicals and clusters.

Although the radiative lifetimes for most vibrationally excited states are expected to be longer than μs , the lifetimes for IVRs can be shorter than ns. For excited vibrational states with IVR lifetime shorter than ns, the IR-VUV-PI and IR-VUV-PFI-PE methods presented here cannot be applied. However, since the IVR lifetime is expected to be longer for lower frequency vibrational states, where the density of states is low, the limitation of short IVR lifetimes can be avoided by selecting excited vibrational modes with lower vibrational frequencies.

In the current IR-VUV-PI and IR-VUV-PFI-PE measurements, a crossed laser-molecular beam configuration is used. The interaction volume for photoionization in this configuration is estimated to be $\approx 2\text{ mm} \times 2\text{ mm} \times 3\text{ mm}$. The sensitivity of PIE, PFI-PE, and PFI-PI measurements using the VUV and IR-VUV photoion-photoelectron detection schemes can be enhanced by increasing the photoionization volume. We have tested a collinear approach for VUV-PIE and VUV-PFI-PE measurements by directing the VUV laser counter propagating to the molecular beam of the sample gas. By this, together with the use of a large MCP, we are able to detect photoions and PFI-PEs formed in a path length of 4 cm at the photoionization region as compared to that of $\approx 3\text{ mm}$ in the crossed VUV-molecular beam arrangement. In this collinear arrangement, the VUV laser radiation is selected by a slightly off-axis biconvex MgF_2 lens and a set of apertures. The signal intensity observed in a VUV-PFI-PE measurement of CH_3I is found to be enhanced by a factor of ≈ 100 as compared to using the crossed VUV-molecular beam arrangement. Although this enhancement factor includes a signal increase of 5–10 fold due to the VUV intensity gain by not using the VUV monochromator, this test experiment indicates that the sensitivity of the IR-VUV-PI and IR-VUV-PFI-PE methods can also be further improved by a similar factor using the collinear arrangement for the IR-VUV lasers and the molecular beam.

In summary, using a broadly tunable single mode IR-OPO laser and a comprehensive tunable VUV laser, together with the molecular beam method, we have shown that the IR-VUV-PI method is a generally applicable, highly sensitive method for IR spectroscopy studies of neutral molecules. The enhanced sensitivity of the IR-VUV-PI method achieved by using the high-resolution, single mode IR-OPO laser translates directly into the high sensitivity for IR-VUV-PFI-PE measurements of cations. The rovibrationally selected and resolved state-to-state PFI-PE spectra thus obtained by the IR-VUV-

PFI-PE method have made possible definitive assignments of photoelectron spectra of the cations of the test molecules. The sensitivity of the experiments demonstrated here shows that there are good prospects for the application of the IR-VUV-PI and IR-VUV-PFI-PE methods for spectroscopy studies of neutral radicals and clusters and their cations.

IV. ACKNOWLEDGMENTS

This work was supported by the NSF (No.CHE0517871). The authors also acknowledge partial support from the DOE Contract (No.DE-FG02-02ER15306), the AFOSR Grant (No.FA9550-06-1-0073) and the NASA Grant (No.07-PATM07-0012).

- [1] X. M. Qian, A. H. Kung, T. Zhang, K. C. Lau, and C. Y. Ng, *Phys. Rev. Lett.* **91**, 233001 (2003).
- [2] H. K. Woo, P. Wang, K. C. Lau, X. Xing, C. Chang, and C. Y. Ng, *J. Chem. Phys.* **119**, 9333 (2003).
- [3] P. Wang, X. Xing, K. C. Lau, H. K. Woo, and C. Y. Ng, *J. Chem. Phys.* **121**, 7049 (2004).
- [4] P. Wang, X. Xing, S. J. Baek, and C. Y. Ng, *J. Phys. Chem. A* **108**, 10035 (2004).
- [5] C. Y. Ng, *J. Electron Spectroscopy & Related Phenomena* **142**, 179 (2005).
- [6] M. K. Bahng, X. Xing, S. J. Baek, and C. Y. Ng, *J. Chem. Phys.* **123**, 084311 (2005).
- [7] M. K. Bahng, X. Xing, S. J. Baek, X. M. Qian, and C. Y. Ng, *J. Phys. Chem. A* **110**, 8488 (2006).
- [8] X. Xing, M. K. Bahng, P. Wang, K. C. Lau, S. J. Baek, and C. Y. Ng, *J. Chem. Phys.* **125**, 133304 (2006).
- [9] X. Xing, B. Reed, K. C. Lau, S. J. Baek, M. K. Bahng, and C. Y. Ng, *J. Chem. Phys.* **127**, 044313 (2007).
- [10] X. Xing, M. K. Bahng, B. Reed, C. S. Lam, K. C. Lau, and C. Y. Ng, *J. Chem. Phys.* **128**, 104306 (2008).
- [11] X. Xing, B. Reed, M. K. Bahng, and C. Y. Ng, *J. Phys. Chem. A* **112**, 2572 (2008).
- [12] J. Keske, D. A. McWhorter, and B. H. Pate, *Int. Rev. Phys. Chem.* **19**, 363 (2000).
- [13] T. L. Tan, S. Y. Lau, P. P. Ong, K. L. Goh, and H. H. Teo, *J. Mol. Spec.* **203**, 310 (2000).
- [14] R. E. Smalley, B. L. Ramakrishna, D. H. Levy, and L. Wharton, *J. Chem. Phys.* **61**, 4363 (1974).
- [15] C. Y. Ng, *Ann. Rev. Phys. Chem.* **53**, 101 (2002).
- [16] X. Xing, B. Reed, M. K. Bahng, P. Wang, and C. Y. Ng, to be published.
- [17] H. K. Woo, J. P. Zhan, K. C. Lau, C. Y. Ng, and Y. S. Cheung, *J. Chem. Phys.* **116**, 8803 (2002).
- [18] H. K. Woo, K. C. Lau, J. P. Zhan, C. Y. Ng, Y. S. Cheung, W. K. Li, and P. M. Johnson, *J. Chem. Phys.* **119**, 7789 (2003).